

# SYNERGISTIC EFFECT OF $Zn^{2+}$ AND ATMP IN CORROSION INHIBITION OF MILD STEEL IN NEUTRAL ENVIRONMENT

S RAJENDRAN AND B V APPARAO

Chemistry Department, Gandhigram Rural Institute, Gandhigram 624302, Tamil Nadu. INDIA

N PALANISWAMY

Central Electrochemical Research Institute, Karaikudi 630 006, Tamil Nadu. INDIA

**Synergistic effect of  $Zn^{2+}$  and sodium salt of aminotrimethylene phosphonic acid (ATMP) in corrosion inhibition of mild steel in water containing low concentration (60 ppm) of Cl<sup>-</sup> has been evaluated by weight loss method. The results show that 98% inhibition efficiency is achieved with the binary system consisting of 200 ppm ATMP and 50 ppm  $Zn^{2+}$ . Potentiostatic polarisation studies show that while ATMP alone acts as anodic inhibitor, ATMP- $Zn^{2+}$  combination acts as mixed inhibitor. The mechanistic aspects of corrosion inhibition and the nature of the film formed on the metal surface have been analysed with the help of UV-Visible reflectance spectra, FTIR spectra, luminescence spectra and XRD patterns. The protective film appears to be consisting of  $Fe^{2+}$ -ATMP complex and  $Zn(OH)_2$  which is also found to be luminescent.**

**Keywords:** Synergistic effect, corrosion inhibition, mixed inhibitor, luminescence and  $Fe^{2+}$ -ATMP complex.

## INTRODUCTION

Several studies on the use of phosphonic acids as corrosion inhibitors have been reported in the literature [1-10]. Even though several papers have discussed the use of aminotrimethylene phosphonic acid (ATMP) as corrosion inhibitor in neutral medium, synergism between ATMP and  $Zn^{2+}$  mechanism of corrosion inhibition and the nature of the film formed on the metal surface have not been studied in detail. In this paper, synergistic effect of ATMP and  $Zn^{2+}$  in corrosion inhibition of mild steel in neutral environment containing 60 ppm chloride ion has been studied by weight loss method and potentiostatic polarisation method. The nature of the film formed on the metal surface has been analysed by recording FTIR spectra, X-ray diffraction (XRD) patterns, UV-Visible reflectance spectra and luminescence emission spectra.

## EXPERIMENTAL

### Preparation of the specimens

For weight loss method and surface examination studies, mild steel specimens (0.02-0.03% S, 0.3-0.8% P, 0.4-0.5% Mn, 0.1-0.2% C and rest Fe) of the dimensions 1 x 4 x 0.2 cm were polished to mirror finish and degreased with trichloroethylene. For potentiostatic polarisation studies, mild steel rod of the above composition encapsulated in teflon with an exposed cross section of 0.5 cm diameter was used as working electrode. Its surface was polished to mirror finish and degreased with trichloroethylene.

### Weight loss method

Mild steel specimens in triplicate were immersed in 100 ml of the test solutions for a period of seven days. The weights of the specimens before and after immersion were determined using Mettler balance, AE-240.

### Potentiostatic polarisation study

This study was carried out in a three electrode cell assembly connected to Bioanalytical system (BAS-100A) electrochemical analyser using mild steel as the working electrode, platinum as the counter electrode and saturated calomel electrode as the reference electrode.

### FTIR Spectroscopic study

The surface film was scratched carefully and the powder obtained was thoroughly mixed so as to make it uniform throughout. FTIR spectrum of the powder (KBr pellet) was recorded using Perkin- Elmer 1600 FTIR spectrophotometer.

### UV-Visible absorption spectroscopy

UV-Visible absorption spectra of aqueous solutions were recorded using Hitachi U-3400 spectrophotometer. The same instrument was used for recording UV-Visible reflectance spectra of the film formed on the metal surface.

### X-ray diffraction technique

The XRD patterns of the film formed on the metal surface were recorded using a computer controller X-ray powder diffractometer, JEOL JDX 8030 with  $Cu K_{\alpha}$  (Ni filtered) radiation ( $\lambda = 1.5418\text{\AA}$ ) at a rating of 40 KV, 20 MA. The scan rate was  $0.05\text{-}20^{\circ}$  per step and the measuring time was 1 sec per step.

### Luminescence spectroscopy

Luminescence spectra of the film formed on the metal surface were recorded using Hitachi 650-10 S fluorescence spectrophotometer equipped with a 150 W Xenon lamp and a Hamamatsu R 929 F photomultiplier tube. The emission spectra were corrected for the spectral response of the photomultiplier tube used.

## RESULTS AND DISCUSSION

### Weight loss method

The formulation consisting of 200 ppm ATMP and 50 ppm  $Zn^{2+}$  offers an inhibition efficiency of 98% (Table I. It is found that 200 ppm ATMP alone has an inhibition efficiency of only 28% and 50 ppm  $Zn^{2+}$  is infact corrosive. But their combination offers 98% inhibition efficiency. This clearly indicates the synergistic effect of ATMP and  $Zn^{2+}$ . It is interesting to note that with higher concentration of  $Zn^{2+}$  greater than 50 ppm in combination with 200 ppm ATMP, inhibition efficiency decreases to low value such as 79%. Thus it is clear that ATMP (200 ppm)- $Zn^{2+}$  (50 ppm) combination is most effective as corrosion inhibitor.

**TABLE I: Corrosion rates of mild steel in chloride environment (60 ppm) and inhibition efficiency of  $Zn^{2+}$ -ATMP combination obtained by weight loss method**

Sl. No.	Concn. of ATMP ppm	Conc. of $Zn^{2+}$ ppm	Corrosion rate, mdd ( $\pm 0.01$ mdd)	Inhibition efficiency %
1.	0	0	15.54	—
2.	10	0	14.76	5
3.	50	0	13.21	15
4.	100	0	12.43	20
5.	150	0	11.66	25
6.	200	0	11.19	28
7.	200	10	10.88	30
8.	200	50	0.31	98
9.	200	100	2.33	85
10.	200	150	3.11	80
11.	200	200	3.11	80
12.	200	300	3.26	79
13.	0	50	19.11	-23

### Potentiostatic polarisation method

It is interesting to note that while ATMP alone acts as anodic inhibitor, ATMP- $Zn^{2+}$  combination acts as mixed inhibitor (Fig. 1).

### Analysis of UV-Visible absorption spectra

This study reveals that new peaks are observed when  $Zn^{2+}$  and ATMP are mixed in solution and also when  $Fe^{2+}$  and ATMP are mixed together (Fig. 2). Increase in absorbance is also noticed in both the cases. These observations indicate the formation of  $Zn^{2+}$ -ATMP complex and also  $Fe^{2+}$ -ATMP complex in solution.

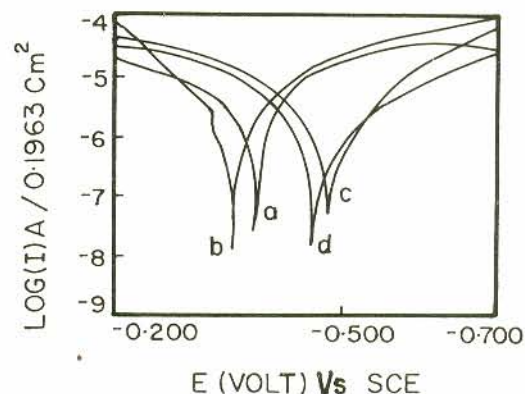


*Fig. 1: Potentiostatic polarisation curves*  
 (a)  $Cl^-$  60 ppm (b)  $Cl^-$  60 ppm + ATMP 200 ppm  
 (c)  $Cl^-$  60 ppm +  $Zn^{2+}$  50 ppm  
 (d)  $Cl^-$  60 ppm + ATMP 200 ppm +  $Zn^{2+}$  50 ppm

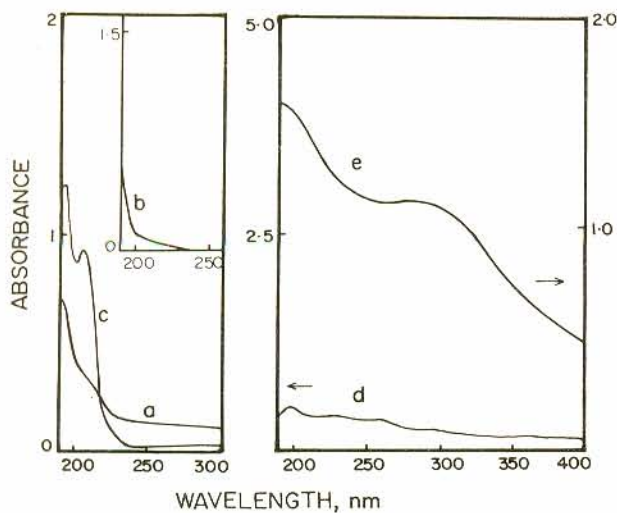


Fig. 2: UV-Visible absorption spectra of solutions  
 (a) ATMP 200 ppm (b)  $Zn^{2+}$  50 ppm  
 (c) ATMP 200 ppm +  $Zn^{2+}$  50 ppm (d)  $Fe^{2+}$  100 ppm  
 (e) ATMP 200 ppm +  $Fe^{2+}$  100 ppm

### Analysis of FTIR spectra

The FTIR spectrum of pure ATMP is given in Fig. 3a. The FTIR spectrum of the film formed on the surface of the metal immersed in 60 ppm  $Cl^-$  and 200 ppm ATMP (Fig. 3b) reveals that the C-N stretching frequency of ATMP in the free state has shifted from  $1145\text{ cm}^{-1}$  to  $1036\text{ cm}^{-1}$  and the P-O stretching frequency has shifted from  $1002\text{ cm}^{-1}$  to  $919$

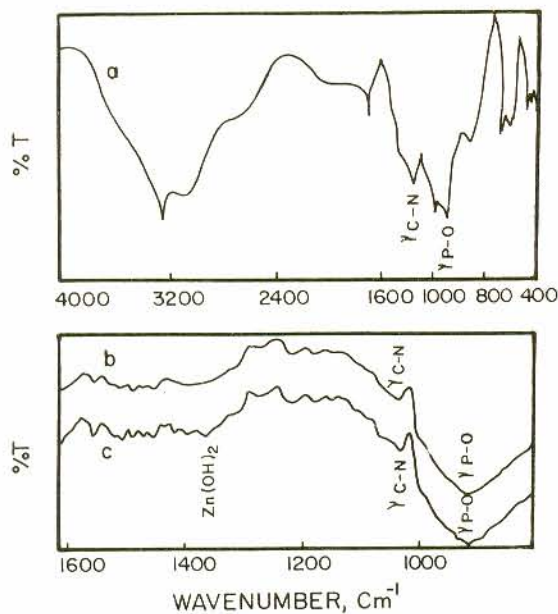


Fig. 3: FTIR spectra

- (a) Pure ATMP  
 (b)  $Cl^-$  60 ppm + ATMP 200 ppm (surface film)  
 (c)  $Cl^-$  60 ppm + ATMP 200 ppm +  $Zn^{2+}$  50 ppm (surface film)

$\text{cm}^{-1}$  [11-14]. These shifts indicate that the N and O atoms are coordinated to  $Fe^{2+}$  [15]. The FTIR spectrum of the film formed on the metal surface immersed in 60 ppm  $Cl^-$ , 200 ppm ATMP and 50 ppm  $Zn^{2+}$  shows that the C-N stretching frequency has shifted from  $1145\text{ cm}^{-1}$  to  $1033\text{ cm}^{-1}$  and the P-O stretching frequency from  $1002\text{ cm}^{-1}$  to  $916\text{ cm}^{-1}$ . These shifts suggest that the N and O atoms are coordinated to  $Fe^{2+}$  in this case also. The band at  $1363\text{ cm}^{-1}$  is due to  $Zn(OH)_2$  [4].

### Analysis of XRD patterns

The XRD patterns of mild steel specimens immersed in various test solutions are given in Figs. 4a-d. With specimen immersed in 60 ppm  $Cl^-$  solution, in addition to iron peaks ( $2\theta=44.7, 65.0$  and  $82.4^\circ$ ), peaks due to magnetite ( $Fe_3O_4$ ) occur at  $2\theta=30.1, 35.5$  and  $62.5$  [16,17]. With the metal immersed in 60 ppm  $Cl^-$  and 50 ppm  $Zn^{2+}$ ,  $Fe_3O_4$  peak occurs at  $2\theta=35.4^\circ$ . With polished specimen, immersed in 60 ppm  $Cl^-$  and 200 ppm ATMP, the peak due to  $\gamma\text{-FeOOH}$  occurs at  $2\theta=33.0^\circ$ . The peaks at  $2\theta=46.8, 59.8$  and  $61.7^\circ$  correspond to  $\gamma\text{-FeOOH}$  and the ones at  $2\theta=37.3$  and  $57.1^\circ$  are due to  $Fe_3O_4$ . With polished mild steel immersed in 60 ppm  $Cl^-$ , 50 ppm  $Zn^{2+}$  and 200 ppm ATMP, no additional peaks other than that of iron occur. This confirms that the metal is completely protected from corrosion and also the protective film does not consist of any oxide of iron.

### Analysis of UV-Visible reflectance spectra

These spectra of the metal surfaces immersed in the test solutions are given in Figs. 5a-d. The reflectance spectra of the metal immersed in 60 ppm  $Cl^-$ , and 200 ppm ATMP, and also in 60 ppm  $Cl^-$  and 50 ppm  $Zn^{2+}$  show the same wavelength transition, namely, at 550 nm. This gives a band

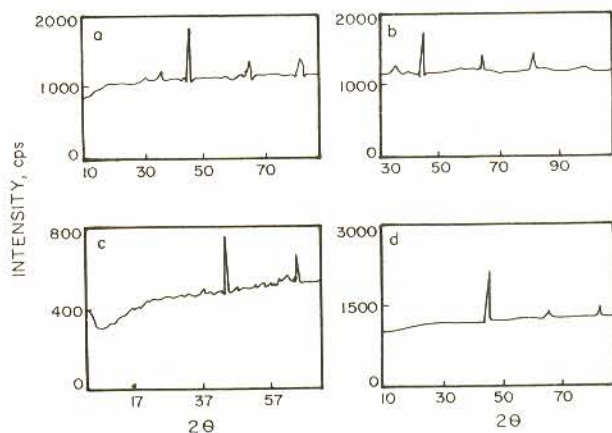


Fig. 4: XRD patterns of surface films

- (a)  $Cl^-$  60 ppm (b)  $Cl^-$  60 ppm +  $Zn^{2+}$  50 ppm  
 (c)  $Cl^-$  60 ppm + ATMP 200 ppm  
 (d)  $Cl^-$  60 ppm + ATMP 200 ppm +  $Zn^{2+}$  50 ppm

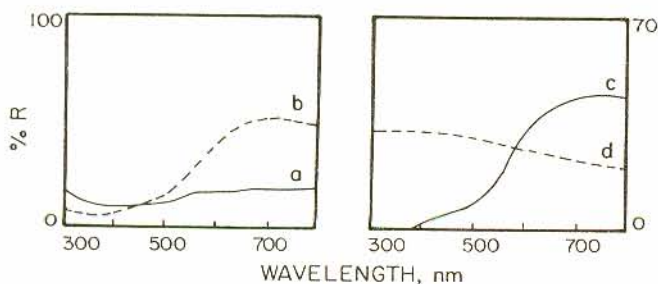


Fig. 5: UV-Visible reflectance spectra of the surface films  
 (a)  $Cl^-$  60 ppm (b)  $Cl^-$  60 ppm + ATMP 200 ppm  
 (c)  $Cl^-$  60 ppm +  $Zn^{2+}$  50 ppm  
 (d)  $Cl^-$  60 ppm + ATMP 200 ppm +  $Zn^{2+}$  50 ppm

gap of 2.25 eV which corresponds to oxides of iron [18,19]. On the other hand the reflectance spectrum for mild steel immersed in 60 ppm  $Cl^-$ , 200 ppm ATMP and 50 ppm  $Zn^{2+}$  (Fig. 5d) does not show any wavelength transition. It is inferred that the surface of the metal is not at all covered by iron oxide. That means whatever action has been brought about by ATMP and  $Zn^{2+}$  separately (Figs. 3b and c) is nullified by the combination of ATMP and  $Zn^{2+}$ .

### Analysis of Luminescence spectra

UV-Visible luminescence emission spectra at  $\lambda_{ex} = 360$  nm are shown in Figs. 6a-c. The spectra for the surface immersed in ATMP alone (Fig. 6a) and for the surface immersed in  $Cl^-$  and ATMP (Fig. 6b) are nearly same while the spectrum of the surface immersed in  $Cl^-$ , ATMP and  $Zn^{2+}$  combination is different from the other two. This indicates that the luminescence emission is due to  $Fe^{2+}$ -ATMP complex embedded in oxides of iron in the former two cases while it is due to  $Fe^{2+}$ -ATMP complex alone in the latter.

### Mechanism of corrosion inhibition

Weight loss method reveals that the formulation consisting of 200 ppm ATMP and 50 ppm  $Zn^{2+}$  offers an inhibition efficiency of 98%. Polarisation study shows that this formulation acts as mixed inhibitor. UV-Visible absorption spectroscopy indicates the possibility of formation of  $Fe^{2+}$ -ATMP complex and also  $Zn^{2+}$ -ATMP complex in solution. FTIR spectra reveal that  $Fe^{2+}$ -ATMP complex and  $Zn(OH)_2$  are present in the protective film on the metal surface. Luminescence spectra reveal that the film formed on the metal surface is luminescent. In order to explain all these observations in a wholistic way, a suitable mechanism of corrosion inhibition is proposed as follows.

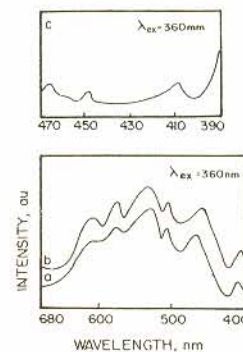


Fig. 6: Luminescence emission spectra of the surface films  
 (a) ATMP 200 ppm  
 (b)  $Cl^-$  60 ppm + ATMP 200 ppm  
 (c)  $Cl^-$  60 ppm + ATMP 200 ppm +  $Zn^{2+}$  50 ppm

1. When the environment consisting of 60 ppm  $Cl^-$  + 200 ppm ATMP + 50 ppm  $Zn^{2+}$  is prepared,  $Zn^{2+}$ -ATMP complex is formed in solution.
2. Now, when the metal is immersed in this environment, the  $Zn^{2+}$ -ATMP complex diffuses from the bulk of the solution to the surface of the metal.
3. On the surface of the metal,  $Zn^{2+}$ -ATMP complex is converted into  $Fe^{2+}$ -ATMP complex in the local anodic region as the latter is more stable than the former.  

$$Zn^{2+} - ATMP + Fe^{2+} \longrightarrow Fe^{2+} - ATMP + Zn^{2+}$$
 Formation of  $Fe^{3+}$ -ATMP complex also to some extent can not be ruled out.
4. The released  $Zn^{2+}$  ions on the surface form  $Zn(OH)_2$  precipitate in the local cathodic regions.  

$$Zn^{2+} + 2OH^- \longrightarrow Zn(OH)_2 \downarrow$$
5. Thus the protective film consists of  $Fe^{2+}$ -ATMP complex and  $Zn(OH)_2$ .

### CONCLUSIONS

1. The formulation consisting of 200 ppm ATMP and 50 ppm  $Zn^{2+}$  offers an inhibition efficiency of 98% in controlling corrosion of mild steel in neutral environment containing 60 ppm  $Cl^-$ .
2. While ATMP alone acts as anodic inhibitor, the ATMP- $Zn^{2+}$  formulation acts as mixed inhibitor.
3. The protective film consists of  $Fe^{2+}$ -ATMP complex and  $Zn(OH)_2$ .
4. The protected metal surface is found to be luminescent.

**Acknowledgement:** S R wishes to thank the Director, CECRI, Karaikudi for permission to work at CECRI and UGC, New Delhi, India for awarding fellowship under FIP.

### REFERENCES

1. P H Ralston, *J Petroleum Technology*, **21** (1969) 1029
2. G B Hatch and P H Ralston, *Mat Prot Perf*, **11** (1972) 39
3. J Kubicki, S Kuczkowska, P Falewicz and B Pyrwano, *Proc 6th Europ Symp on Corrosion Inhibitors*, Ferrara, **2** (1985) 1131
4. I Sekine and Y Kirakawa, *Corrosion*, **42** (1986) 272
5. A John Mikroyanidis, *Phosphorus Sulphur*, **32** (1987) 113
6. P Sullivan and A Yeoman, *Proc Int Water Conf Eng Soc*, West Pa, **49th** (1988) 435
7. D Vanloyan, *Werkstoffe und Korrosion*, **40** (1989) 599
8. D Vanloyan and G Zocher, *Werkstoffe und Korrosion*, **41** (1990) 613.
9. Yu I Kuznetsov and A F Raskolnikov, *Zashch Metal*, **28** (1992) 249
10. E Kalman, B Varhegyi, I Bako, I Felhosi, F H Karman and A Shaban, *J Electrochem Soc*, **141** (1994) 3357
11. A D Cross, *"Introduction to practical infra-red spectroscopy"*, Butterworths Scientific Publication, London (1990) p 73
12. R M Silverstein, G Clayton Bassler and Terence C Morrill, *"Spectrometric Identification of Organic Compounds"*, John Wiley Sons, New York (1981) 166
13. J L Fang, Y Li, X R Ye, Z W Wang and Q Liu, *Corrosion*, **49** (1993) 266
14. Kazuo Nakamoto, "Infrared and Raman spectra of Inorganic and Coordination compounds", *Wiley Interscience*, New York (1986) 168
15. T D J Smith, *Inorg Nucl Chem*, **9** (1959) 150
16. M Favre and D Landolt, *Proc 7th Europ Symp on Corrosion Inhibitors*, Ferrara, **2** (1990) 787
17. M Favre and D Landolt, *Corrosion Science*, **34** (1993) 1481
18. G Lfoley, J Krugen and C J Bechtold, *J Electrochem Soc*, **114** (1967) 936
19. M Sharon, G Tamizhmani and K Basaraswaran, *Proc Indian Nat Sci Acad*, **52** (1986) 311